Structural and optical properties of annealed W-doped $BaTiO_3$ thin films prepared by pulsed laser deposition

2007 J. Phys.: Condens. Matter 19 466214

(http://iopscience.iop.org/0953-8984/19/46/466214)

IOP PUBLISHING JOURNAL OF PHYSICS: CONDENSED MATTER

J. Phys.: Condens. Matter **19** (2007) 466214 (11pp) doi:10.1088/0953-8984/19/46/466214

Structural and optical properties of annealed W-doped $BaTiO_3$ thin films prepared by pulsed laser deposition

A Y Fasasi[1,2,3,7], R Bucher[2], B D Ngom[4], U Buttner[5], M Maaza[2], C Theron[2] and E G Rohwer[6]

[1] Centre for Energy Research and Development, Obafemi Awolowo University, Ile-Ife, Osun State, Nigeria
[2] iThemba Labs, National Research Foundation, Somerset West, Cape Town, South Africa
[3] African Laser Centre (ALC), South Africa
[4] Groupe de Physique des Solides et Sciences des Matériaux, Faculté des Sciences et Techniques, Université Cheikh Anta Diop, Dakar, Senegal
[5] Department of Electrical Engineering, University of Stellenbosch, Stellenbosch, South Africa
[6] Laser Research Institute, Department of Physics, University of Stellenbosch, Stellenbosch, South Africa

E-mail: ayfasasi@yahoo.co.uk

Received 4 July 2007, in final form 5 October 2007
Published 25 October 2007
Online at stacks.iop.org/JPhysCM/19/466214

Abstract

Tungsten-doped barium titanate thin films have been prepared on glass and silicon substrates by laser ablation. The films were compositionally, structurally and optically characterized. Rutherford backscattering spectroscopy simulation gave the composition to be $Ba_{0.85}W_{0.05}Ti_{0.94}O_{3.2}$ with a cationic ratio $(Ba + W)/Ti$ of 0.95. All the films without annealing were amorphous. The calculated lattice constants through the diffraction patterns on the silicon substrate indicated the high probability of the film having a cubic symmetry. Atomic force microscopy results showed the film surface to be smooth with a maximum roughness of 5 nm, varied grain size distribution and average grain size of 50 nm. Through the Swanepoel envelope method, the refractive index dispersion was obtained. Maximum and minimum refractive indices of 2.6 and 2.32 at 475 and 812 nm, respectively, were calculated. Analysis of the dependence of the refractive index and the dielectric constant on wavelength led to the determination of the high-frequency dielectric constant (ε_∞) and the carrier density effective mass ratio (N_c/m^*). The single-oscillator model proved to be adequate for describing the dispersion behaviour. Through this model, the dispersion parameter, average oscillator parameter and strength were determined. The optical band gap obtained on annealed sample was 3.8 eV by assuming a direct transition.

(Some figures in this article are in colour only in the electronic version)

[7] Author to whom any correspondence should be addressed.

1. Introduction

Barium titanate, a perovskite material with the chemical formula $BaTiO_3$, has been extensively studied in bulk and thin film forms [1–6] due to its interesting properties. It is ferroelectric, piezoelectric as well as pyroelectric [7]. It has a high dielectric constant [8] and its optical non-linearity makes it a good candidate for optoelectronic applications [9, 10]. Further improvements of these functional qualities have been given a lot of attention through the introduction of transition metal and rare-earth oxides as dopants to substitute for either Ti or Ba in the $BaTiO_3$ lattice. Incorporation of transition metal oxides has been studied in the bulk form to observe the influence of these additions on the electrical and dielectric properties such as the electrical resistivity, dielectric constant, passage from normal ferroelectric to relaxor-type transition [11–13] and positive temperature coefficient of resistivity (PTCR) effect [14, 15]. On the other hand, the effect of the addition of rare-earth oxides to $BaTiO_3$ has also been studied in the bulk as well as in thin film form using different film growth techniques [3, 4, 16]. In the thin film form of rare-earth-doped $BaTiO_3$, studies have centred mostly on photoluminescence and non-linear optical properties [17, 18].

Tungsten oxide (WO_3) is another material that is widely employed for its electrochromicity [19], as a sensor material for gas sensing [20, 21] and in optical data storage and switching [22]. Despite these characteristics, WO_3 has not been actively employed as a dopant in $BaTiO_3$, either in bulk or thin film form. Therefore, the aims of the present study are to increase the amount of information already in existence on $BaTiO_3$ by preparing thin films of W-doped $BaTiO_3$ on glass and silicon substrates using pulsed laser ablation and to study their structural and optical properties. To the best of our knowledge, this is the first time that the optical properties W-doped $BaTiO_3$ thin film have been studied. The surface of the films has been studied by atomic force microscope (AFM) while the structure of the films has been looked at using x-ray diffraction analysis. The composition and the thickness of the films have been determined by Rutherford backscattering spectroscopy (RBS) and the room temperature transmittance in the wavelength range 400–900 nm has been employed to determine the refractive index dispersion and its associated parameters such as oscillator and dispersion energy, oscillator strength and zero-frequency as well as high-frequency dielectric constant.

2. Experimental procedure

WO_3, TiO_2 and BaO powders were all purchased from Alfa Aesar with percentage purities of 99.8, 99.9 and 97 respectively. The BaO powder contained 97% BaO and 2.6% $BaCO_3$. According to the certificate of analysis of the oxides, the impurities present in WO_3 are less than 10 parts per million (ppm) while those present in TiO_2 are no greater than 0.006 wt%.

The powders were weighed in the right proportion to obtain films having compositions with the following formula: $Ba_{1-x}W_xTiO_3$. The powders were thoroughly mixed in a mortar and pre-sintered in air at 400 °C for 3 h. The dried mixture was again re-ground and pressed with a load of 20×10^3 kg using a manual hydraulic press to obtain a disc shape of 13 mm diameter and various thicknesses. Sintering was carried out at a maximum temperature of 1150 °C with a dwell time of $3\frac{1}{2}$ h, at the end of which the sample was allowed to cool down to room temperature before removal.

Laser ablation was performed with an excimer laser having a wavelength of 308 nm at a frequency of 16 Hz under pulsed oxygen. The employment of pulsed oxygen during the deposition helped to increase the film thickness and also served to minimize droplet formation (the mechanism of which is currently not well understood). Preliminary studies showed that

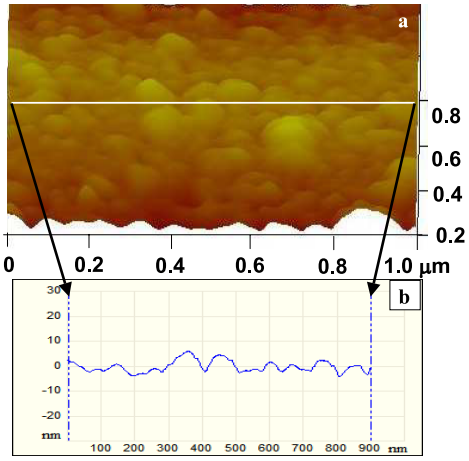

Figure 1. Surface characterization by AFM. (a) Three-dimensional view of the surface of W-doped $BaTiO_3$ annealed film on Corning glass substrate and (b) surface roughness analysis of the white section in two-dimensional view.

the experimental conditions necessary to obtain smooth and adherent films are the use of a base pressure of 5×10^{-2} Pa, substrate–target distance of 60 mm, substrate temperature of 400 °C and oxygen pressure of 5 Pa at a pulse rate of 1.6 ms with a constant deposition time of 60 min on Corning glass and silicon substrates. The target was rotated to maintain the shape and size of the plume throughout the period of ablation.

Annealing of the samples was effected in argon gas containing 9.7 mol% hydrogen and 1 ppm oxygen. Films on glass substrates were annealed at a temperature of 450 °C while those on silicon were annealed at 800 °C for a constant dwell time of 6 h at a heating and cooling rate of 5 °C min^{-1}.

The surface characteristics of the films were studied with the aid of a NanoMan V Veeco atomic force microscope (AFM) while the AFM images were analysed with Nanoscope V700 software. The structures of the films were determined by x-ray diffraction analysis carried out with an x-ray diffractometer (model Bruker AXS D8 Advance) at the iThemba LABS in South Africa. The transmission spectra were collected between 200 and 900 nm with a Varian UV–visible spectrometer (model Cary 1E) which covers the ultraviolet (200–400 nm), visible (400–800 nm) and the near-infrared (800–900 nm) regions. Fourier transform infrared transmission (FTIR) measurements were also carried out in the wavenumber range 400–4000 cm^{-1} with a Perkin-Elmer FTIR spectrometer (model Paragon 1000PC). To find the compositions of the films, an RBS study was undertaken. For this purpose, a $4He^{2+}$ ion beam generated from a van de Graaff accelerator was used as the projectile. The scattering angle was 165° and the resolution of the detector was 20 keV. During the process of acquiring the spectral data, the energy of the ion beam used was 2 MeV. All the spectra were analysed using the free RBS analysis software RUMP.

3. Results and discussion

3.1. Atomic force microscopy (AFM)—surface observation

A typical result obtained from the measurement of the surface roughness of the annealed W-doped $BaTiO_3$ films on glass substrates by AFM is shown in figure 1, where it can be seen

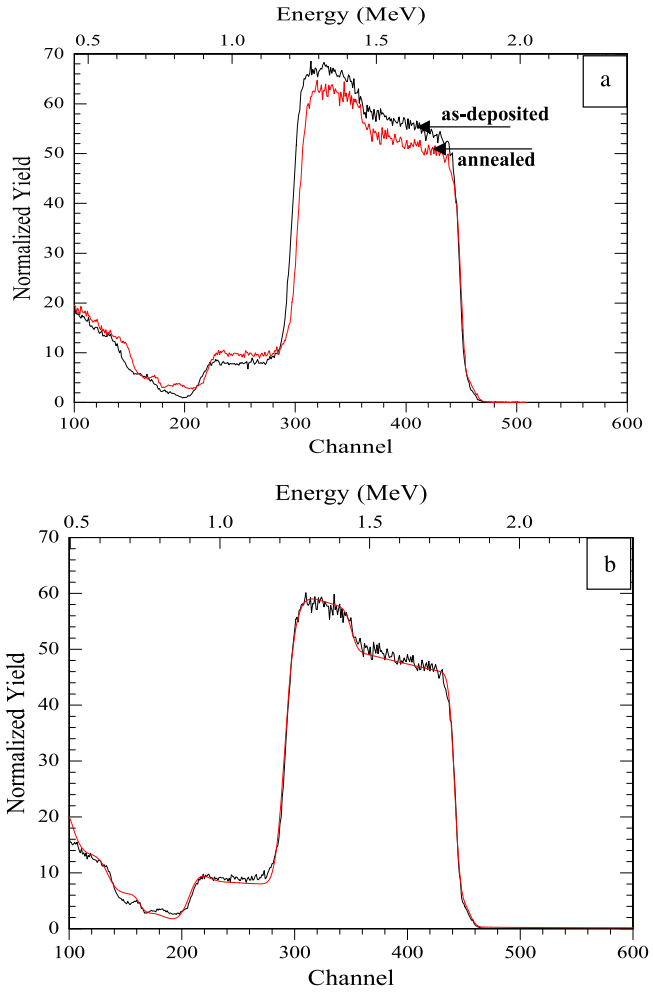

Figure 2. (a) Comparison between the RBS spectrum of as-deposited and annealed films of tungsten-doped $BaTiO_3$ deposited on Corning glass substrate and (b) fitting of the RBS spectrum of the annealed W-doped $BaTiO_3$ on glass using RUMP software.

that the surface is relatively flat and smooth with the film consisting of grains of different size distribution (figure 1(a)). The maximum surface roughness plot (measured across the white line in figure 1(a)) presented in figure 1(b), shows the maximum roughness to be about 5 nm. The average grain size measured was 50 nm.

3.2. RBS analyses—composition and film thickness

RBS, apart from giving the composition and hence the stoichiometry of the films, also indicated that annealing of the film on Corning glass substrates led to a decrease in film thickness (figure 2(a)), which may probably be due to a reduced film porosity leading to a more compact film. The abrupt fall of the Ti profile towards lower energy indicates that the film has a smooth surface. No chemical diffusion features between the substrate and the film were observed. Normalization of the concentration so that the sum of the elemental fraction is equal to 5 leads

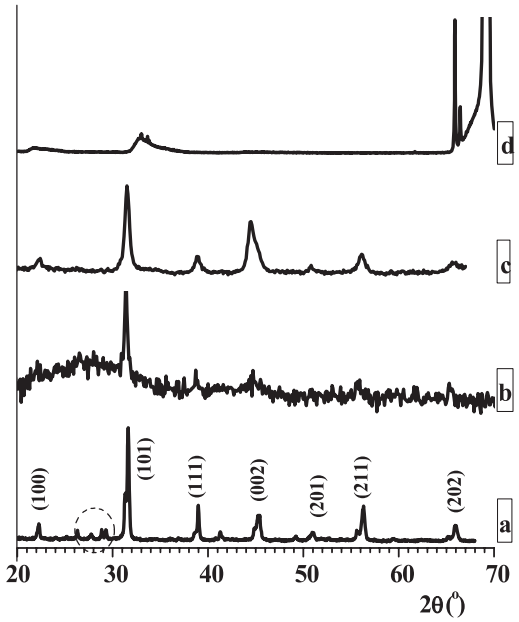

Figure 3. X-ray diffraction patterns of W-doped $BaTiO_3$ (a) pellet, (b) thin film on Corning glass substrate, (c) thin film on silicon substrate and (d) pure silicon for comparison.

to the film having the composition $Ba_{0.85}W_{0.05}Ti_{0.94}O_{3.2}$ with a cationic ratio (Ba + W)/Ti of 0.95 which is smaller than the ideal stoichiometric ratio of 1. Mounaix *et al* [23] also observed that the best crystallized films in the $BaSrTiO_3$ system maintained a (Ba + Sr)/Ti ratio which is notably lower than the value of 1. They ascribed this non-stoichiometry to possible segregation of titanium oxide phases along the grain boundaries which cannot be resolved by RBS. In addition, Chety *et al* [24], in their study of $GdCa_4O(BO_3)_3$ thin film, observed a strong dependence of the Ca/Gd ratio on oxygen pressure, which is typical of complex oxides. Their observation was explained by both the sticking coefficient connected with the volatility of the species which are incorporated in the film during growth and the different spatial distribution of the species in the plume during laser ablation. Apart from these two possible causes of non-stoichiometry, cation vacancy formation may also have played an important role.

3.3. X-ray diffraction analyses—structural determination

The results of the x-ray diffraction analyses of W-doped $BaTiO_3$ pellets employed for ablation, films on glass and silicon substrates are shown in figures 3(a)–(d). The diffraction peaks of the pellet show some unidentified peaks. These peaks, which are encircled in figure 1(a), may be due to the impurities present in the starting oxides employed in forming the titanate. Apart from these unidentified peaks, all the other peaks correspond to the major peaks of the tetragonal phase of $BaTiO_3$. Comparing the intensities of the unidentified peaks with the $BaTiO_3$ peaks, one observes that these unidentified peaks represent about 10% of the total number of peaks, which is probably an indication that the percentage of the $BaTiO_3$ phase in the pellet is about 90%. The diffraction pattern of the annealed film on glass substrate, presented in figure 1(b), indicates that the film has a preferred orientation in the (101) crystallographic direction. The

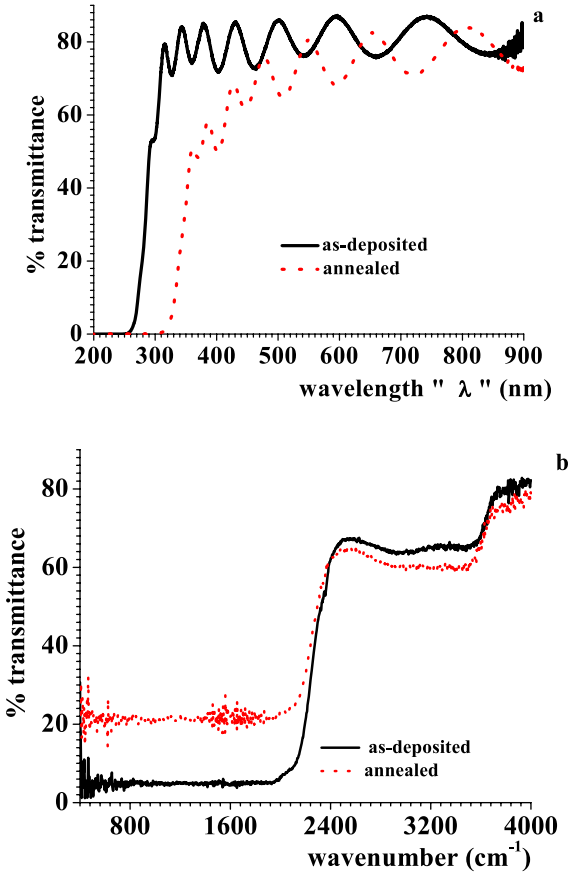

Figure 4. Typical optical transmission spectra of annealed and as-deposited W-doped $BaTiO_3$ deposited on glass: (a) UV–visible spectra and (b) FTIR spectra.

positive effect of increased annealing temperature on the crystallinity of the film is shown in figure 3(c) for film grown on silicon and annealed at 800 °C. The film on the silicon substrate manifests a better crystallinity than the film on the glass substrate. Moreover, comparison between figures 3(c) and (d) shows the absence of silicon diffraction peaks on figure 3(c), which is an indication of a relatively thick film. On both glass and silicon substrates, the unidentified peaks have disappeared, which is probably due to the small thickness of the films. All the as-prepared films were amorphous. The lattice constants calculation using the (101) and (111) peaks with a Cu Kα source ($\lambda = 1.5417$ Å) on the silicon substrate gave 'a' and 'c' to be 4.008 ± 0.005 and 4.003 ± 0.005 Å, respectively. This may probably signify that the film has a cubic symmetry.

3.4. Optical properties

Optical characterization was performed on samples deposited on Corning glass substrates. Typical UV–visible transmission spectra of samples of both annealed and as-deposited films of W-doped $BaTiO_3$ (figure 4(a)) show a percentage transmittance of well over 80%. The presence of interference fringes is an indication of a thicker film with a smooth surface. The smoothness of the surface is corroborated by the AFM result in figure 1(a). A sharp fall in transmission

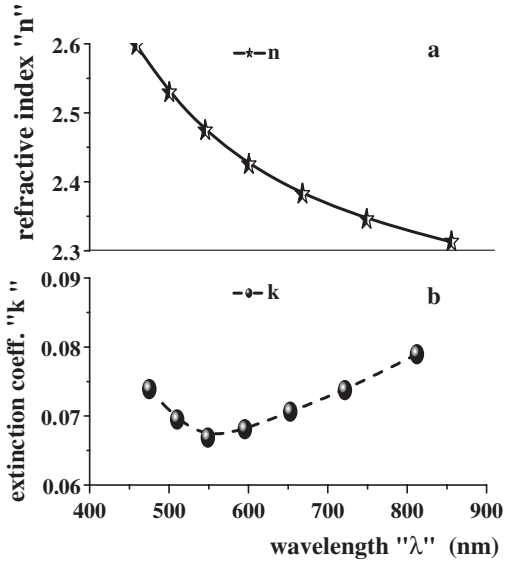

Figure 5. Plot of (a) the refractive index and (b) the extinction coefficient for annealed W-doped $BaTiO_3$ deposited on a glass substrate.

at 295 and 360 nm for as-deposited and annealed film on the glass substrate indicates a single transition in the UV region for WO_3-doped $BaTiO_3$. This sharp fall in transmission suggests similar distribution of energies among the grains in the film. There is a cut-off wavelength shift from 260 to 320 nm due to annealing. With FTIR (figure 4(b)), the transmittance shows a varied dependence on photon energy. Above 3700 cm^{-1} there is a slight difference between the transmittance of the annealed and as-deposited samples which is close to 80%. Between 2480 and 3500 cm^{-1}, there is a drop in transmittance to 60 and 67% for annealed and as-deposited samples, respectively. In the region between 400 and 2000 cm^{-1}, there is a marked difference in the transmittance; 5% for as-deposited and 22% for annealed samples. The high transmittance of the annealed sample at low wavenumber is probably an indication of redistribution of defects inside the film due to annealing.

The interference fringes observed in the films have been employed to determine the variation of refractive index with wavelength using the Swanepoel envelope method. With the film thickness determined through RBS, the absorption and the extinction coefficients [25] can be obtained as a function of wavelength through the use of equations (1) and (2)

$$\alpha = \frac{1}{t} In\left(\frac{1}{T}\right) \tag{1}$$

$$k = \frac{\alpha\lambda}{4\pi}, \tag{2}$$

where 't' is the film thickness of the annealed sample and 'T' is the percentage transmittance. The variation of refractive index and extinction coefficient of the annealed W-doped $BaTiO_3$ as a function of wavelength is presented in figure 5. The refractive index decreases gradually from 2.6 at 476 nm to 2.32 at 812 nm while the extinction coefficient shows a decrease from $k = 0.07$ at 473 nm to $k = 0.06$ at 550 nm and a gradual increase to 0.08 at 813 nm. In all the wavelength ranges considered, n is greater than k.

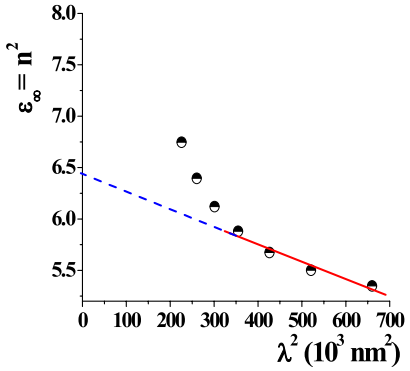

Figure 6. Plot to determine the high-frequency dielectric constant ε_∞ of W-doped $BaTiO_3$ thin film on a glass substrate.

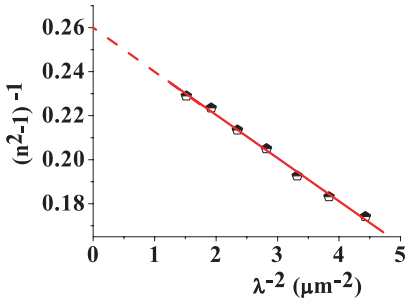

Figure 7. Plot to determine the average oscillator strength and oscillator parameter for W-doped $BaTiO_3$ thin film on a glass substrate.

With the value of n much greater than k, then $\varepsilon' \approx n^2$ and the dependence of ε' on λ can be examined using equation (3) [25]

$$\varepsilon' = n^2 = \varepsilon_\infty - \left(\frac{e^2}{\pi c^2}\right)\left(\frac{N_c}{m^*}\right)\lambda^2. \tag{3}$$

In this expression, e is the electronic charge, c is the speed of light, N_c is the carrier density, m^* is the effective mass of the carrier and ε_∞ is the high-frequency dielectric constant. From the plot of n^2 as a function of λ^2, the intersection at $\lambda^2 = 0$ for the linear part of the curve at higher wavelength gives the high-frequency dielectric constant ε_∞ while the slope gives the N_c/m^* ratio. Figure 6 shows such a plot where the values of $\varepsilon_\infty = 6.43$ and $N_c/m^* = 1.87 \times 10^{49}$ were obtained.

Different Sellmier dispersion expressions exist to explain the variation of refractive index with wavelength, but the most typical is to use the long wavelength approximation of the single-term Sellmier relation (equation (4)) which retains the physical significance of the oscillator parameters. The single-term Sellmier relation is given as [26–29]

$$n^2(\lambda) - 1 = \frac{S_o\lambda_o^2}{[1 - (\frac{\lambda_o}{\lambda})^2]}, \tag{4}$$

where λ_o is the average oscillator parameter and S_o is the average oscillator strength. The plot of $(n^2(\lambda) - 1)^{-1}$ as a function of λ^{-2} gives a straight line (figure 7) where the values of $1/S_o$ and $1/\lambda_o^2 S_o$ can be evaluated from the slope and the intercept, respectively. The dispersion

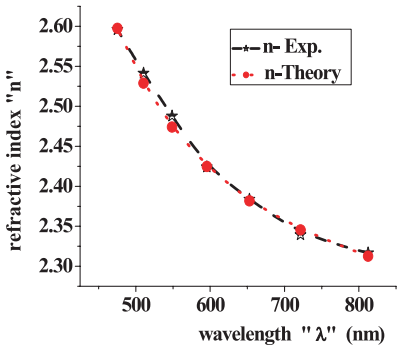

Figure 8. Comparison between the experimental points and the theoretical points obtained from using the determined values of S_o and λ_o on W-doped $BaTiO_3$ thin film on a glass substrate.

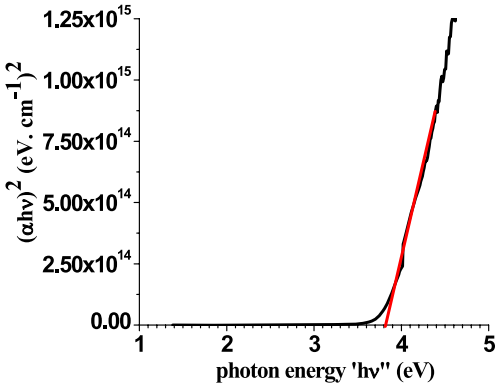

Figure 9. Plot for determining the optical band gap of annealed W-doped $BaTiO_3$ film deposited on a Corning glass substrate.

parameter (E_o/S_o with $E_o = \eta c/e\lambda_o$) can also be determined. The values of λ_o, S_o and E_o/S_o determined are 0.275 μm, 5.1×10^{13} m^{-2} and 1.41×10^{-14} eV m^2, respectively. Substitution of the values of S_o and λ_o into equation (4) will permit the replotting of the refractive index with wavelength. The replotting is shown in figure 8. It can be seen that there is good agreement between the experimental points and the values obtained using S_o and λ_o. This shows that the single-oscillator model is adequate to describe the dispersion behaviours of this material in the low absorption region of the transmission spectra.

When the valence and the conduction band densities of states are parabolic, the absorption coefficient α and photon energy are related by equation (5) [30]

$$\alpha(E) = B\frac{(h\nu - E_g)^m}{h\nu}, \tag{5}$$

where $h\nu$ is the photon energy, E_g is the optical band gap and m is a power factor which can be 1/2 or 2 for direct and indirect band gap materials, respectively. A plot of $(\alpha h\nu)^2$ versus $h\nu$ is presented in figure 9 for annealed W-doped $BaTiO_3$ where the extrapolation of the linear part of the absorption spectrum to zero gives the optical band gap to be 3.8 eV. Our calculated band gap is 0.2 eV greater than that of $BaTiO_3$ single crystal [31] and close to the value for bulk $BaTiO_3$ [32] reported as 3.72 eV. It has been observed in many studies that the value of the optical band gap of thin films is process dependent as well as grain size dependent. Mansingh

et al [33] observed a variation in optical band gap as well as lattice constants as a function of substrate to target distance in rf-sputtered ITO films. Also, Suzuki *et al* [27] observed low band gap energy of 3.47 eV on $BaTiO_3$ thin film prepared by radio-frequency-plasma CVD with a grain size of 6.7 nm. Apart from these dependences, we strongly believe that W addition may have contributed to the difference in band gap energy between the value reported in this study and the bulk $BaTiO_3$ value.

4. Conclusion

W-doped $BaTiO_3$ thin films have been prepared using pulsed laser deposition. Atomic force microscopy study of the films revealed the surface to be smooth and uniform with a surface roughness of 5 nm. The chemical composition of the films determined by RBS through RUMP software simulation gave almost stoichiometric $Ba_{0.85}W_{0.05}Ti_{0.94}O_{3.2}$ with a cationic ratio (Ba + W)/Ti of 0.95. The cationic ratio of less than 1 is an indication of the existence of cation vacancies in the film. All the as-deposited films were amorphous. Highly crystalline films were obtained after annealing at 800 °C on with lattice constants $a = 4.008$ and $c = 4.003$ Å on silicon substrates, which is probably an indication of a cubic phase.

Optical characterization showed the films to be highly transparent with transmittance greater than 80%. This high transmittance makes the films efficient window materials. There is a cut-off wavelength shift from 260 to 320 nm due to annealing. The absence of absorption in the region that lies between 300 and 900 nm is important since it is one of the key requirements for materials having non-linear optical properties (NLO). The high refractive index of the films makes them suitable for employment as anti-reflection coatings. The refractive index dispersion had been analysed and fitted with a single-oscillator model to determine the high-frequency dielectric constant ($\varepsilon_\infty = 6.43$), the carrier density effective mass ratio ($N_c/m^* = 1.87 \times 10^{49}$), the dispersion parameter ($E_o/S_o = 1.41 \times 10^{-14}$ eV m^2), average oscillator parameter ($\lambda_o = 0.275$ μm) and the average oscillator strength ($S_o = 5.1 \times 10^{13}$ m^{-2}). The calculated band gap, assuming direct transition was 3.8 eV making W-doped $BaTiO_3$ a probable candidate for optoelectronic applications.

Acknowledgments

A Y Fasasi wishes to thank the African Laser Centre for meeting the financial and moral commitments necessary for undertaking this project. He would also like to show his appreciation to the staff of iThemba LABS, National Research Foundation, Somerset West and Physics Department, Laser Research Institute, University of Stellenbosch, Stellenbosch, South Africa.

References

[1] Al-Allak H M, Brinkman A W, Russel G J, Roberts A W and Wood J 1988 *J. Phys. D: Appl. Phys.* **21** 1226
[2] Illingsworth J, Al-Allak H M and Brinkman A W 1990 *J. Phys. D: Appl. Phys.* **23** 971
[3] Thomas R, Varadan V K, Kormaneni S and Dube D C 2001 *J. Appl. Phys.* **90** 1480
[4] Roy D and Krupanidhi S B 1992 *Appl. Phys. Lett.* **16** 2057
[5] Sreenivas K, Mansingh A and Sayer M 1987 *J. Appl. Phys.* **62** 4475
[6] Yeh M H, Liu Y C, Liu K S, Lin I N, Lee J Y M and Cheng H F 1993 *J. Appl. Phys.* **74** 2143
[7] Elliot S R 1998 *The Physics and Chemistry of Solids* (England: Wiley)
[8] Saad M M, Baxter P, Bowman R M, Gregg J M, Morrison F D and Scott J F 2004 *J. Phys.: Condens. Matter* **16** L451

[9] Rakuljic G A 1987 *PhD Thesis* California Institute of Technology p 1728 (Source: Dissertation Abstracts International, vol 48-06, Section B)
[10] Yu J, Sun J, Chu J and Tang D 2000 *Appl. Phys. Lett.* **77** 2807
[11] Yoon S H and Kim H 2002 *J. Appl. Phys.* **92** 1039
[12] Wang X, Gu M, Yang B, Zhu S and Cao W 2003 *Microelectron. Eng.* **66** 855
[13] Anwar S, Sagdeo P R and Lalla N P 2006 *J. Phys.: Condens. Matter* **18** 3455
[14] Chao C T, Cann D P, Gall R B and Palaci Y 2004 *J. Phys. D: Appl. Phys.* **37** 416
[15] Kim D-H, Um W-S and Kim H-G 1996 *J. Mater. Res.* **11** 2002
[16] Aal A A, Rashad M M and Amin G A 2007 *J. Phys.: Condens. Matter* **61** 1
[17] Zhang M-S, Zhang W-F, Zhang J, Zhang P and Yin Z 2003 *Proc. SPIE* **4797** 293
[18] Liu Y, Chen Z, Li C, Cui D, Zhou Y, Yang G and Zhu Y 1997 *J. Appl. Phys.* **81** 6328
[19] Djaoued Y, Ashrit P V, Badilescu S and Brüning R 2003 *J. Sol–Gel Sci. Technol.* **28** 235
[20] Wang G, Ji Y, Huang X, Yang X, Gouma P I and Dudley M 2006 *J. Phys. Chem.* B **110** 23777
[21] Rossinyol E, Marsal A, Arbiol J, Peiro F, Cornet A, Morante J R, Tian B, Bo T and Zhao D 2005 *Sensors Actuators* B **109** 57
[22] Bussjager R, Osman J M, Voss E and Chaiken J 1999 *Aerospace Conf. 1999*; *Proc. IEEE* **3** 343
[23] Mounaix P, Tondusson M, Sarger L, Michau D, Reymond V and Maglione M 2005 *Japan. J. Appl. Phys.* **44** 5058
[24] Chety R, Millon E, Boudrioua A, Loulergue J C, Dahoun A and Perriere J 2001 *J. Mater. Chem.* **11** 657
[25] Sati D C, Kumar R and Mehra R M 2006 *Turk. J. Phys.* **30** 519
[26] Girgis S Y, Salem A M and Selim M S 2007 *J. Phys.: Condens. Matter* **19** 116213
[27] Teng C W, Muth J F, Ozgur U, Bergman M J, Everitt H O, Sharma A K, Jin C and Narayan J 2000 *Appl. Phys. Lett.* **76** 979
[28] Sun X W and Kwok H S 1999 *J. Appl. Phys.* **86** 408
[29] DiDomenico M and Wemple S H 1969 *J. Appl. Phys.* **40** 720
[30] Cetinorgu E, Goldsmith S and Boxman R L 2007 *J. Phys.: Condens. Matter* **19** 256206
[31] Kamalassanan M N and Chandra S 1991 *Appl. Phys. Lett.* **59** 3547
[32] Suzuki K and Kijima K 2005 *Japan. J. Appl. Phys.* **44** 2081
[33] Mansingh A and Kumar C V R V 1989 *J. Phys. D: Appl. Phys.* **22** 455